

Robust Detection and Estimation of Change-Points in a Time Series of Multivariate Images

Ammar Mian*,†, Jean-Philippe Ovarlez†,‡, Guillaume Ginolhac† and Abdourahmane M. Atto†

*: CentraleSupélec/SONDRA, Plateau du Moulon, 3 rue Joliot-Curie, F-91190 Gif-sur-Yvette, France

†: ONERA, DEMR/TSI, Chemin de la Hunière, F-91120 Palaiseau, France

‡: LISTIC, Université de Savoie Mont-Blanc, F-74944, Annecy le Vieux, France

Objectives

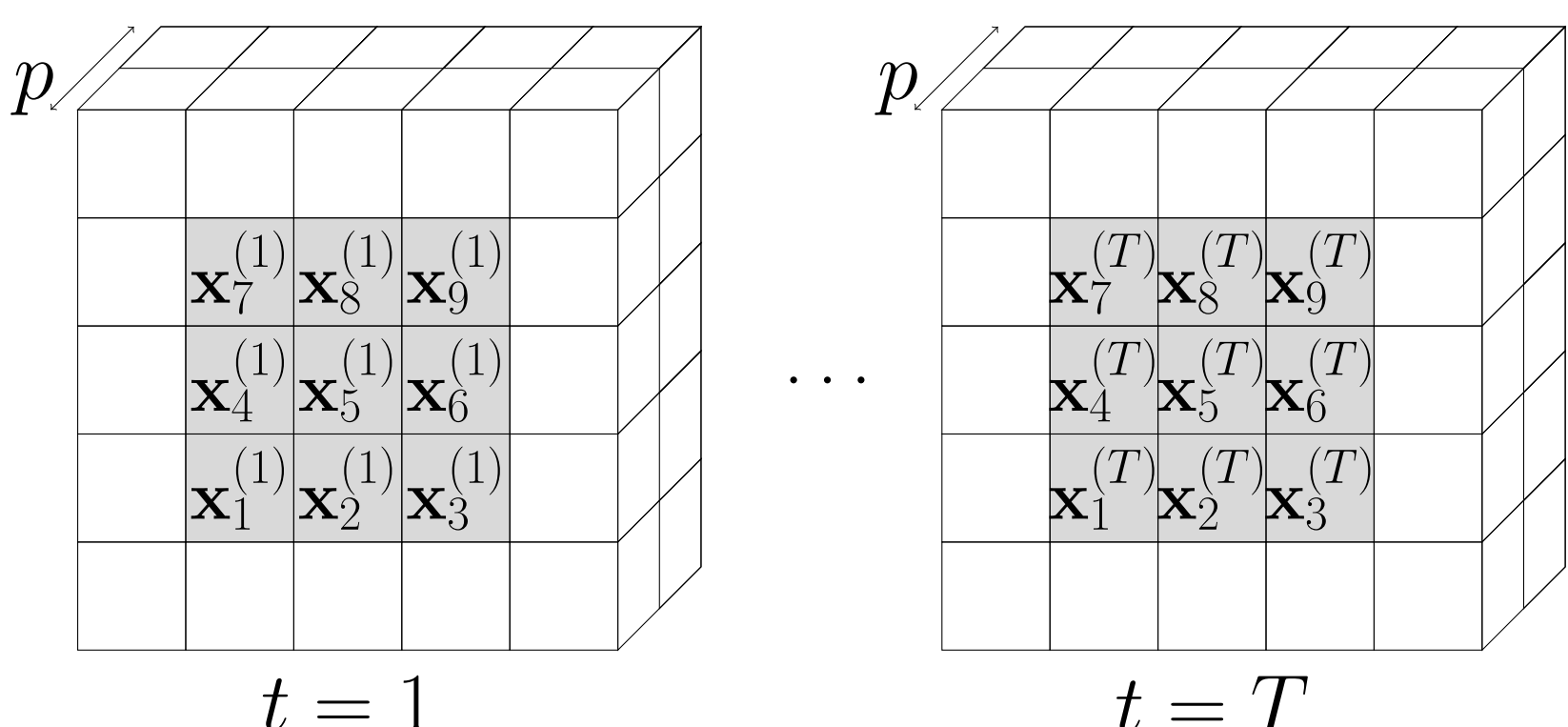
The present paper deals with the joint detection and estimation of change-points in an Image Time Series (ITS) of complex multivariate images. In peculiar, we deal with the heterogeneous behaviour observed in High-Resolution (HR) images which cannot be modelled by a Gaussian model.

To this end, an extension of Conradsen et al.'s work is considered under the large family of Complex Elliptical Symmetric (\mathbb{CE}) distributions. New statistics have been derived using Generalised Likelihood Ratio Test (GLRT) technique and integrated in the estimation algorithm. Simulations show a more robust behaviour and better performance than the Gaussian-derived statistics when the data is heterogeneous.

Introduction

Recent years have seen an increase in the number of remotely sensed images, such as SAR or Hyperspectral images, available to the research communities. Time Series consist in a huge amount of data which cannot be processed by hand. In this context, non supervised methodologies have to be developed for an extensive analysis of change-points.

The data to consider is as follows:



The problem considered presently is:

Consider a Time Series of random vectors $\mathbf{x}^{(t)} \sim p_{\mathbf{x}}(\mathbf{x}; \boldsymbol{\theta}_t)$; given N independent observations $\{\mathbf{x}_k^{(t)}\}_{k=1..N}$, find all $t_C \in \llbracket 2, T \rrbracket$ so that $\boldsymbol{\theta}_{t-1} \neq \boldsymbol{\theta}_{t_C}$. The number of total changes is unknown.

Recently, Conradsen et al. have developed a joint detection and estimation technique using a Gaussian assumption for the local observed pixels ($\boldsymbol{\theta}_t$ is the covariance matrix in this case).

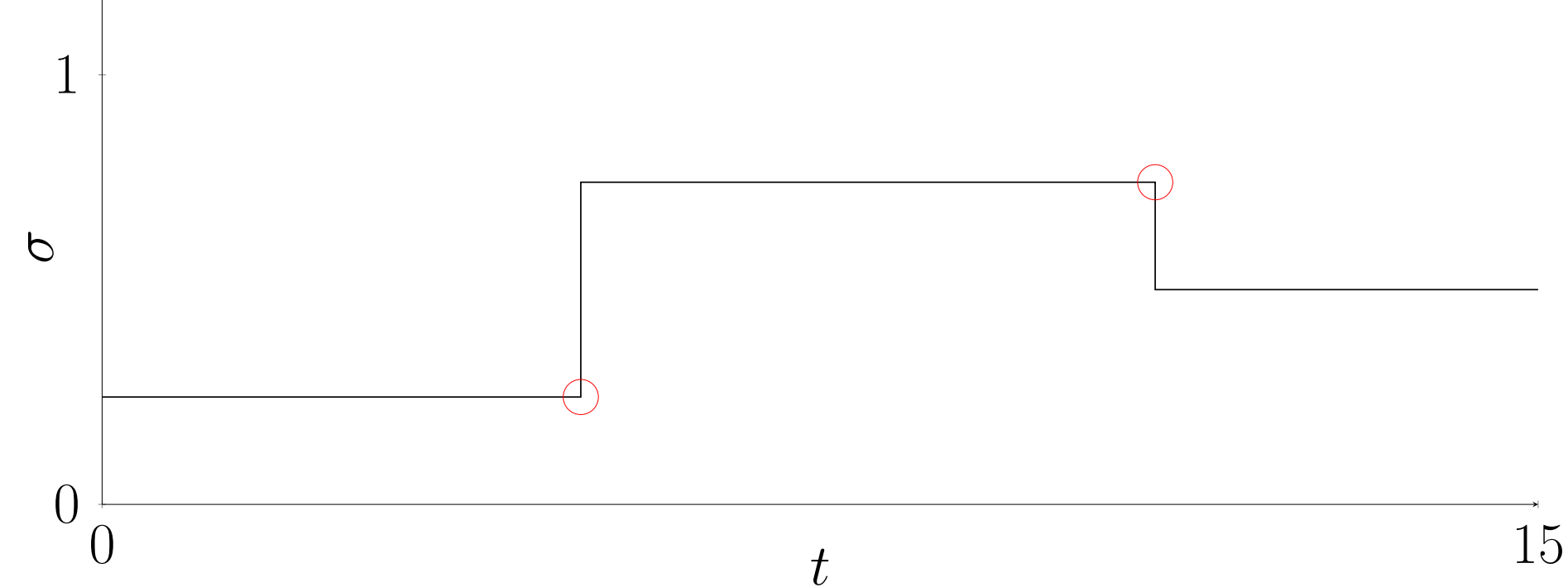


Figure 1: Example with $p = 1, N = 1$.

Omnibus and Marginal schemes

Suppose the local observations $\mathbf{x}_k^{(t)}$ follow an arbitrary model $p_{\mathbf{x}}(\mathbf{x}; \boldsymbol{\theta}_t)$. Two detection schemes are needed:

- Omnibus scheme:

Let $(t_1, t_2) \in \llbracket 1, T \rrbracket^2$, so that $t_2 > t_1$,

$$\begin{cases} H_{0,\text{omni}}^{t_1, t_2} : \boldsymbol{\theta}_{t_1} = \dots = \boldsymbol{\theta}_{t_2} = \boldsymbol{\theta}_{t_1, t_2} \\ H_{1,\text{omni}}^{t_1, t_2} : \exists (t, t') \in \{t_1, \dots, t_2\}^2, \boldsymbol{\theta}_t \neq \boldsymbol{\theta}_{t'} \end{cases} \quad (1)$$

- Marginal scheme:

Consider $(t_1, t_2) \in \llbracket 1, T \rrbracket^2$, so that $t_2 > t_1$,

$$\begin{cases} H_{0,\text{marg}}^{t_1, t_2} : \boldsymbol{\theta}_{t_1} = \dots = \boldsymbol{\theta}_{t_2-1} = \boldsymbol{\theta}_{t_1, t_2-1} \text{ and } \boldsymbol{\theta}_{t_2-1} = \boldsymbol{\theta}_{t_2} \\ H_{1,\text{marg}}^{t_1, t_2} : \boldsymbol{\theta}_{t_1} = \dots = \boldsymbol{\theta}_{t_2-1} = \boldsymbol{\theta}_{t_1, t_2-1} \text{ and } \boldsymbol{\theta}_{t_2-1} \neq \boldsymbol{\theta}_{t_2} \end{cases} \quad (2)$$

The algorithm

```

1: Initialize  $t_1 \leftarrow 1$ 
2: while  $H_{1,\text{omni}}^{t_1, T}$  do ▷ Omnibus test
3:   Initialize  $r \leftarrow 1$ 
4:   while  $H_{0,\text{marg}}^{t_1, t_1+r}$  do ▷ Marginal tests
5:     Update  $r \leftarrow r + 1$ 
6:   end while
7:   Store  $t_1 + r - 1$  as a change point
8:   Update  $t_1 \leftarrow t_1 + r$ 
9: end while

```

Our contribution

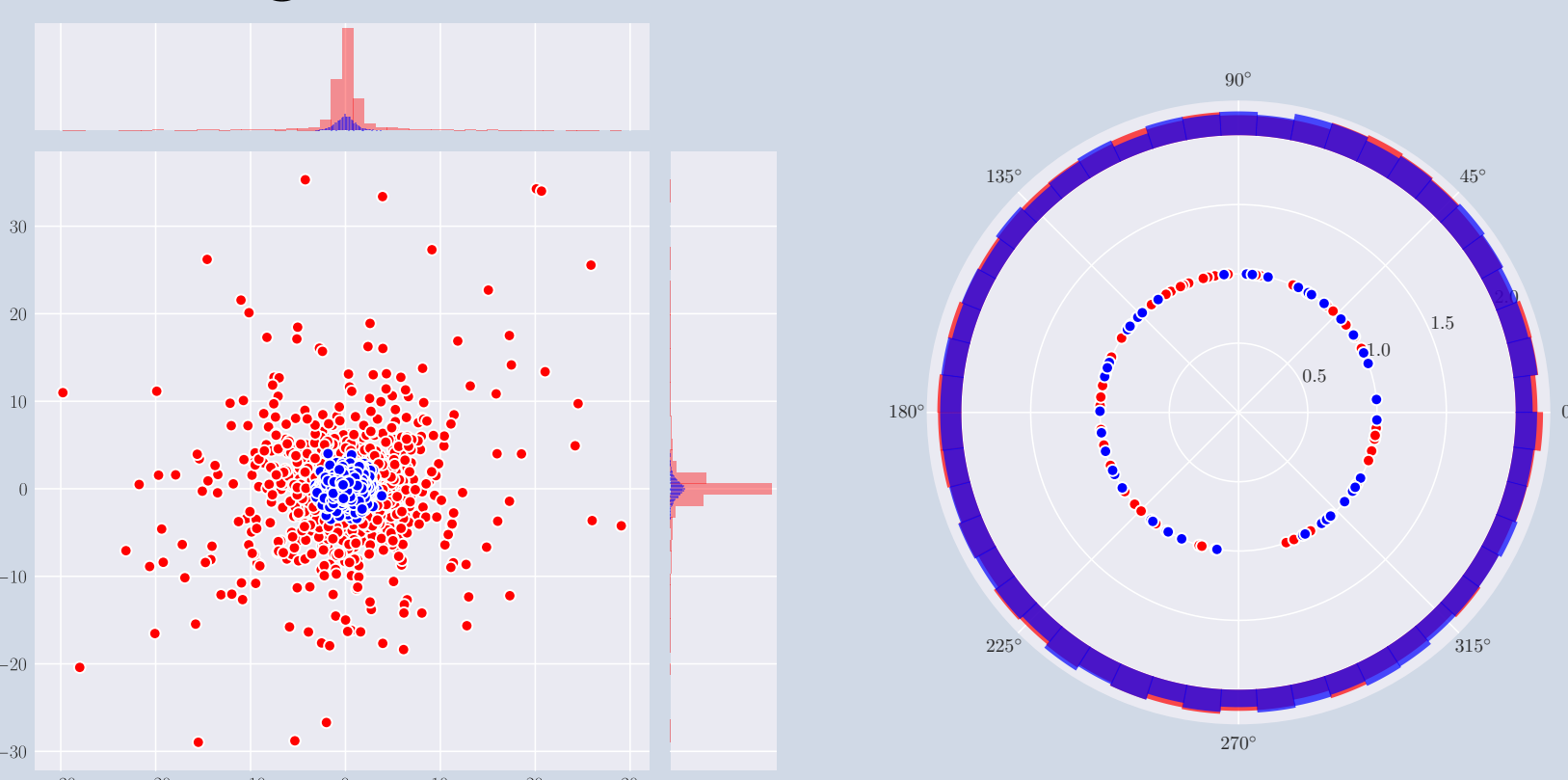
In HR images, the homogeneity on the window is not respected as well as the Gaussian hypothesis and local variations of power are observed. The \mathbb{CE} family, which is more suited to model the observations, is considered.

In peculiar, we consider the self-normalised observations $\mathbf{z}_k^{(t)} = \mathbf{x}_k^{(t)} / \|\mathbf{x}_k^{(t)}\|$ which follows a \mathbb{CAE} distribution:

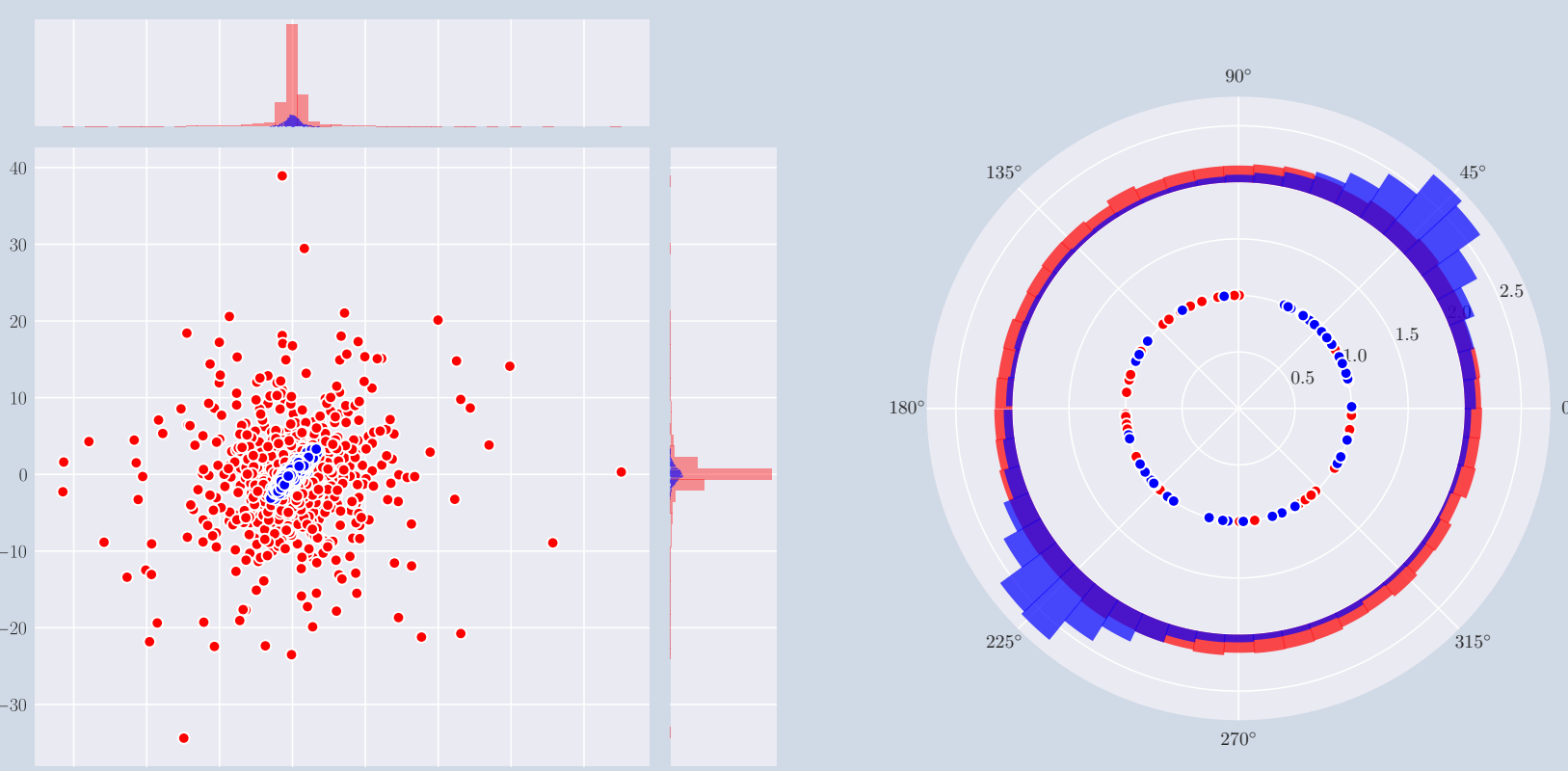
$$p_{\mathbf{z}}^{\mathbb{CAE}}(\mathbf{z}; \Sigma') = \mathfrak{S}_p^{-1} |\Sigma'|^{-1} (\mathbf{z}^H \Sigma'^{-1} \mathbf{z})^{-p}, \quad (3)$$

where $\mathfrak{S}_p = 2\pi^p / \Gamma(p)$ and Γ is the gamma function. The derivation of statistics for problems (1) and (2) are done using $\boldsymbol{\theta}_t = \{\Sigma_t'\}$ and the PDF (3).

- No change scenario:



- Change scenario:



Derivation of new statistics:

- Omnibus Scheme (1):

$$\hat{\Lambda}_{\mathbb{CAE}, \text{omni}}^{t_1, t_2} = \frac{|\hat{\Sigma}_{t_1, t_2}^{\text{TE}}|^{(t_2-t_1)N}}{\prod_{t=t_1}^{t_2} |\hat{\Sigma}_t^{\text{TE}}|^N} \prod_{t=t_1}^{t_2} \prod_{k=1}^N \left(\mathbf{z}_k^{(t)} \mathbf{z}_k^{(t)H} [\hat{\Sigma}_{t_1, t_2}^{\text{TE}}]^{-1} \mathbf{z}_k^{(t)} \right)^p. \quad (4)$$

- Marginal Scheme (2):

$$\begin{aligned} \hat{\Lambda}_{\mathbb{CAE}, \text{marg}}^{t_1, t_2} = & \frac{|\hat{\Sigma}_{t_1, t_2}^{\text{TE}}|^{(t_2-t_1)N}}{|\hat{\Sigma}_{t_2}^{\text{TE}}|^N |\hat{\Sigma}_{t_1, t_2-1}^{\text{TE}}|^{(t_2-t_1-1)N}} \times \\ & \prod_{k=1}^N \left(\prod_{t=t_1}^{t_2-1} \left(\mathbf{z}_k^{(t)} \mathbf{z}_k^{(t)H} [\hat{\Sigma}_{t_1, t_2-1}^{\text{TE}}]^{-1} \mathbf{z}_k^{(t)} \right)^p \right) \left(\mathbf{z}_k^{(t_2)} \mathbf{z}_k^{(t_2)H} [\hat{\Sigma}_{t_2}^{\text{TE}}]^{-1} \mathbf{z}_k^{(t_2)} \right)^p, \end{aligned} \quad (5)$$

with:

$$\forall t, \hat{\Sigma}_t^{\text{TE}} = \frac{p}{N} \sum_{k=1}^N \frac{\mathbf{z}_k^{(t)} \mathbf{z}_k^{(t)H}}{\mathbf{z}_k^{(t)H} [\hat{\Sigma}_t^{\text{TE}}]^{-1} \mathbf{z}_k^{(t)}}. \quad (6)$$

$$\hat{\Sigma}_{t_1, t_2}^{\text{TE}} = \frac{p}{(t_2-t_1)N} \sum_{k=1}^N \sum_{t=t_1}^{t_2} \frac{\mathbf{z}_k^{(t)} \mathbf{z}_k^{(t)H}}{\mathbf{z}_k^{(t)H} [\hat{\Sigma}_{t_1, t_2}^{\text{TE}}]^{-1} \mathbf{z}_k^{(t)}}. \quad (7)$$

Simulation parameters

α, β	ρ_t	p	N	T
Shape and Scale for Γ -distribution	Coefficients for Toeplitz matrices	Size of vector	Number of observations	Number of Images

The new statistics have been tested in simulation and compared to the Gaussian ones. The model used is $\mathbf{x} = \sqrt{\tau} \tilde{\mathbf{x}}$ where $\tau \sim \Gamma(\alpha, \beta)$ and $\tilde{\mathbf{x}} \sim \mathcal{CN}(\mathbf{0}_p, \Sigma)$. The covariance matrices are chosen to be Toeplitz of the form $\Sigma_t(m, n) = \rho_t^{|m-n|}$. ρ_t is the sole parameter governing the change over time.

CFAR property

The new statistics have the texture and scatter matrix Constant False Alarm Rate (CFAR) property. This means that it is possible to guarantee a probability of false alarm P_{FA} by appropriately selecting a threshold !

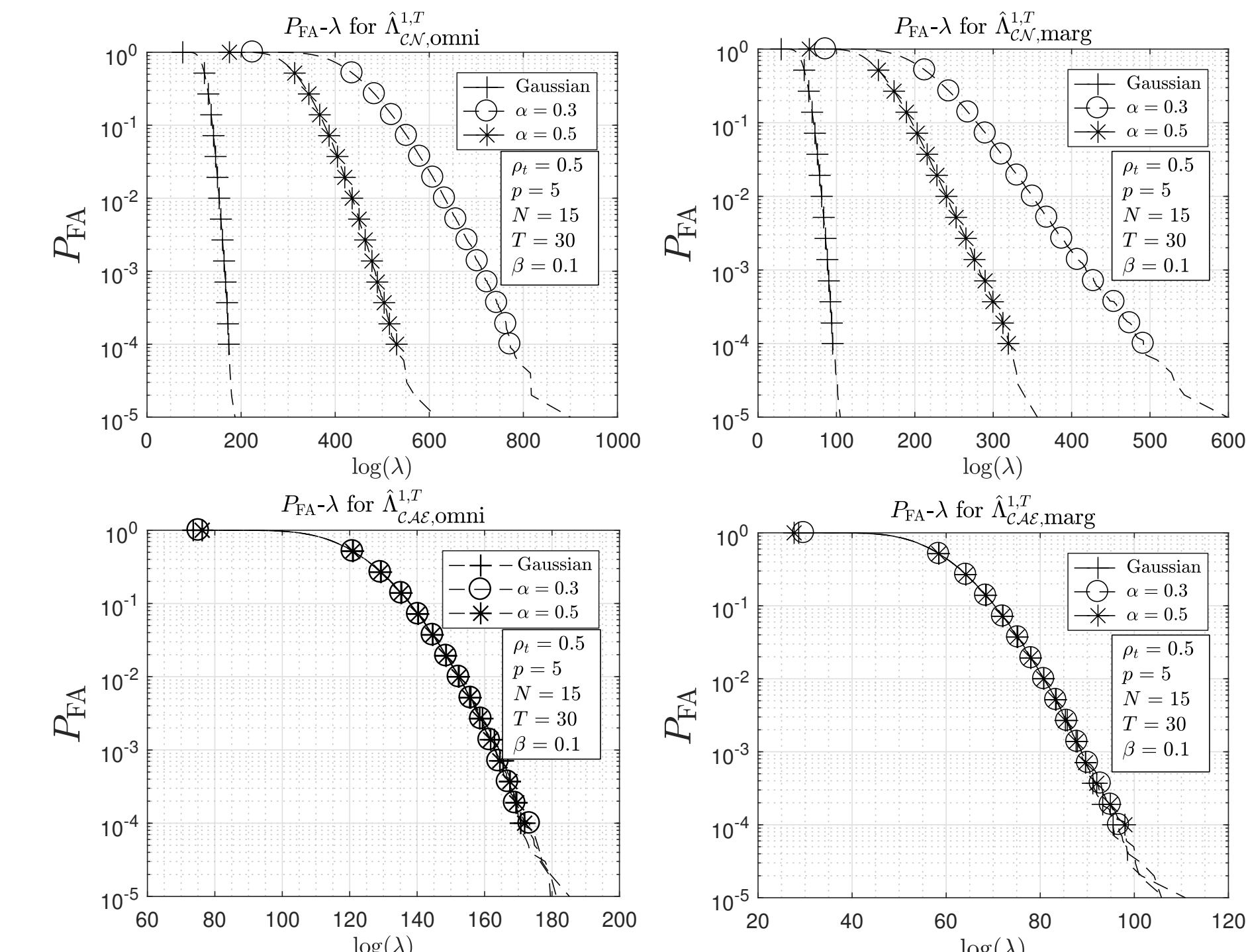
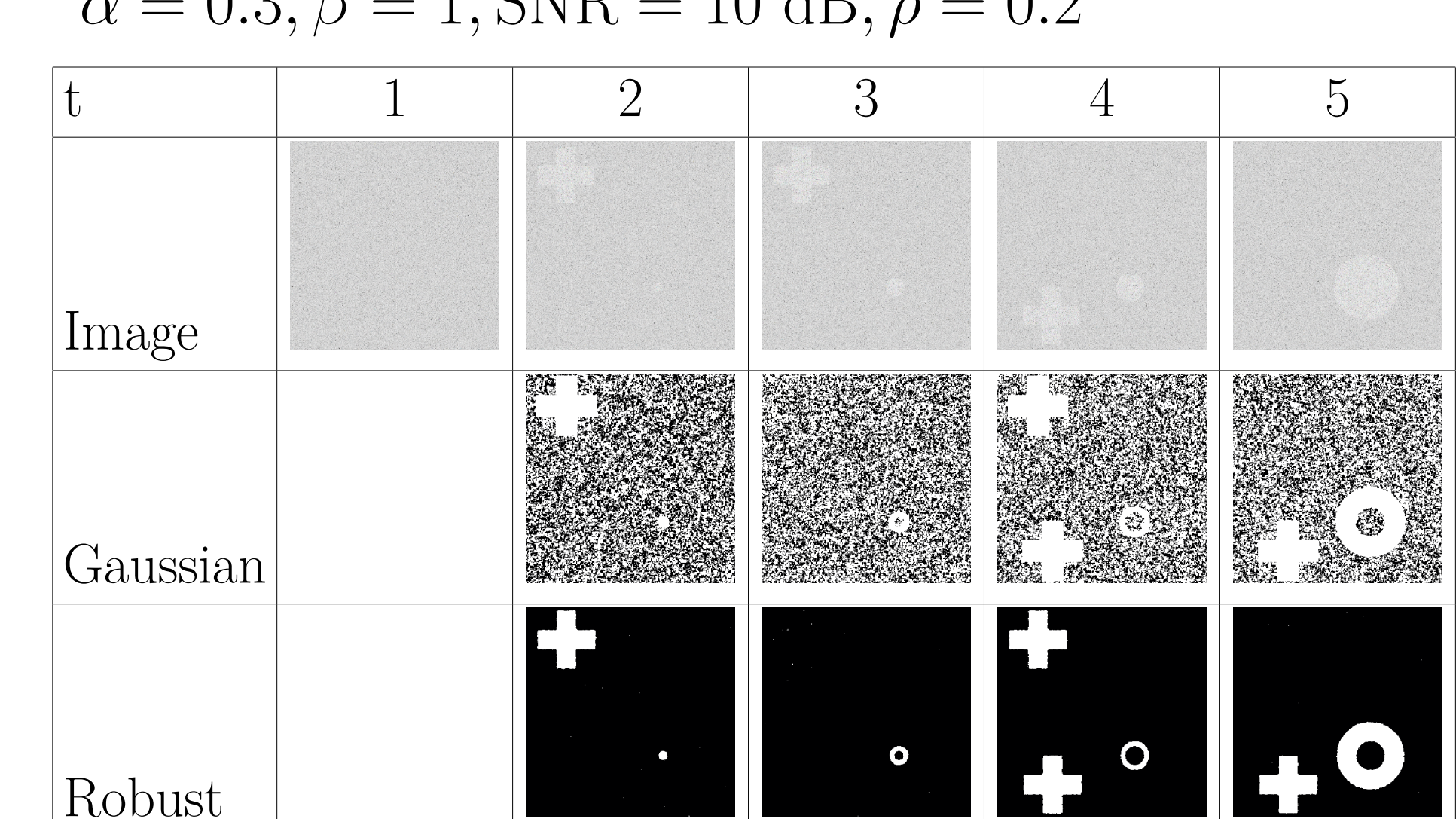


Figure 2: $P_{\text{FA}} - \lambda$ relationships for several parameters of a \mathbb{CCG} distribution under H_0 regime.

Results on synthetic images

Example using $T = 5, p = 3, N = 25, P_{\text{FA}} = 10^{-4}$.

- Background: $\alpha = 0.3, \beta = 0.1, \rho = 0.99$.
- Cross-pattern: $\alpha = 0.3, \beta = 1, \text{SNR} = 10 \text{ dB}, \rho = 0.3$.
- Circle pattern: $\alpha = 0.3, \beta = 1, \text{SNR} = 10 \text{ dB}, \rho = 0.2$.



Conclusions

- New statistics have been derived to using a \mathbb{CE} distribution model.
- They have a more robust behaviour (less false alarms) and better performance of detection for heterogeneous data.
- Perspectives: Try them on real SAR or hyperspectral dataset.